JACC: CLINICAL ELECTROPHYSIOLOGY
VOL. 4, NO. 1, 2018

ISSN 2405-500X/$36.00
PUBLISHED BY ELSEVIER
https://doi.org/10.1016/j.jacep.2017.10.010

Multimodal Examination of Atrial Fibrillation Substrate

Correlation of Left Atrial Bipolar Voltage Using Multi-Electrode Fast Automated Mapping, Point-by-Point Mapping, and Magnetic Resonance Image Intensity Ratio

Tarek Zghaib, MD,[a] Ali Keramati, MD,[a] Jonathan Chrispin, MD,[a] Dong Huang, MD,[a] Muhammad A. Balouch, MD,[a] Luisa Ciuffo, MD,[a] Ronald D. Berger, MD, PhD,[a,b] Joseph E. Marine, MD,[a] Hiroshi Ashikaga, MD, PhD,[a,b] Hugh Calkins, MD,[a] Saman Nazarian, MD, PhD,[c] David D. Spragg, MD[a]

ABSTRACT

OBJECTIVES The aim of this study was to examine atrial fibrillation (AF) substrate using different modalities (point-by-point [PBP], fast anatomic mapping [FAM], and late gadolinium enhancement [LGE] magnetic resonance imaging [MRI] mapping) in patients presenting for AF ablation.

BACKGROUND Bipolar voltage mapping, as part of AF ablation, is traditionally performed in a PBP approach using single-tip ablation catheters. Alternative techniques for fibrosis delineation include FAM with multi-electrode circular catheters and LGE MRI. The correlation between PBP, FAM, and LGE-MRI fibrosis assessment is unknown.

METHODS LGE MRI was performed pre-ablation in 26 patients (73% men, mean age 63 ± 8 years). Local image intensity ratio (IIR) was used to normalize myocardial intensities. PBP and FAM voltage maps were acquired, in sinus rhythm, prior to ablation and coregistered with LGE MRI.

RESULTS The mean bipolar voltage for all 19,087 FAM voltage points was 0.88 ± 1.27 mV, and the average IIR was 1.08 ± 0.18. In an adjusted mixed-effects model, each unit increase in local IIR was associated with a 57% decrease in bipolar voltage ($p < 0.0001$). An IIR >0.74 corresponded to a bipolar voltage <0.5 mV. A total of 1,554 PBP mapping points were matched to the nearest FAM point. In an adjusted mixed-effects model, log FAM bipolar voltage was significantly associated with log PBP bipolar voltage ($\beta = 0.36$; $p < 0.0001$). At low voltages, FAM distribution was shifted to the left compared with PBP mapping; at intermediate voltages, FAM and PBP voltages were overlapping; and at high voltages, FAM voltages exceeded PBP voltages.

CONCLUSIONS LGE-MRI, FAM, and PBP mapping showed good correlation in delineating electroanatomic AF substrate. Each approach has fundamental technical characteristics, the awareness of which allows proper assessment of atrial fibrosis. (J Am Coll Cardiol EP 2018;4:59–68) © 2018 by the American College of Cardiology Foundation.

From the [a]Division of Cardiology, Johns Hopkins University School of Medicine, Baltimore, Maryland; [b]Biomedical Engineering, The Johns Hopkins University, Baltimore, Maryland; and the [c]Division of Cardiology, University of Pennsylvania Perelman School of Medicine, Philadelphia, Pennsylvania. This study was funded by the National Institutes of Health (grants K23HL089333 and R01HL116280) and by a grant from Biosense Webster to Dr. Nazarian; the Roz and Marvin H. Weiner and Family Foundation; the Dr. Francis P. Chiaramonte Foundation; Marilyn and Christian Poindexter; and the Norbert and Louise Grunwald Cardiac Arrhythmia Research Fund. Dr. Nazarian is principal investigator for research funding to Johns Hopkins University from Biosense Webster; and has served as a scientific advisor to Biosense Webster, CardioSolv, and St. Jude Medical. All other authors have reported that they have no relationships relevant to the contents of this paper to disclose.
All authors attest they are in compliance with human studies committees and animal welfare regulations of the authors' institutions and Food and Drug Administration guidelines, including patient consent where appropriate. For more information, visit the *JACC: Clinical Electrophysiology* author instructions page.

Manuscript received June 21, 2017; revised manuscript received October 5, 2017, accepted October 12, 2017.

JACC: CLINICAL ELECTROPHYSIOLOGY VOL. 4, NO. 1, 2018
JANUARY 2018:59–68

ABBREVIATIONS AND ACRONYMS

3D = 3-dimensional

AF = atrial fibrillation

EAM = electroanatomic mapping

FAM = fast anatomic mapping

GEE = generalized estimating equation

IIR = image intensity ratio

LA = left atrial

LGE = late gadolinium enhancement

MRI = magnetic resonance imaging

PBP = point-by-point

PV = pulmonary vein

Pulmonary vein (PV) isolation by radiofrequency ablation has emerged as an effective treatment for atrial fibrillation (AF) by interrupting signal conduction arising from ectopic triggers in the PVs to the left atrial (LA) myocardium (1). Atrial myocardial substrate including areas with low bipolar voltage, shortened effective refractory periods, and conduction heterogeneity all likely play a role in AF perpetuation (2–4). These regional disparities in myocardial properties are thought to support reentry and triggered activity in the atrium (5). Assessment of atrial fibrosis burden is increasingly used for prognostication and to inform ablation strategies (6–8).

SEE PAGE 69

Initial studies examining low-voltage substrate and its correlation with late gadolinium enhancement (LGE) magnetic resonance imaging (MRI) used a point-by-point (PBP) mapping approach using ablation catheters (6,7). Although this approach offers the advantage of confirming tissue contact using force-sensing catheters, it is time-consuming. An alternative is fast anatomic mapping (FAM) using decapolar circular mapping catheters (CARTO LASSO 2515 Variable Loop Eco Nav, Biosense Webster, Diamond Bar, California) with a smaller electrode size that can acquire highly detailed (>1,000 points) voltage maps in significantly less time. However, the correlation of LA fibrosis detected with LGE MRI, PBP mapping, and FAM is unknown. Voltage correlation between these techniques has not been established despite the use, in clinical practice, of common voltage thresholds (0.2 to 0.5 mV) to define diseased myocardium irrespective of the mapping technique. In this study, we sought to examine and compare AF substrate characteristics using different modalities (LGE MRI, FAM, and PBP mapping) in patients presenting for AF ablation.

METHODS

PATIENT POPULATION. Twenty-six patients with symptomatic, drug-refractory paroxysmal or persistent AF referred for AF ablation underwent preprocedural MRI between June 2016 and December 2016. The Johns Hopkins Institutional Review Board approved the study, and all patients provided written informed consent for both the ablation procedure and inclusion in medical research at the time of the procedure.

MRI ACQUISITION. Images were obtained using a 1.5-T MRI scanner (Avanto, Siemens, Erlangen, Germany) and a 6-channel phased-array body coil in combination with a 6-channel spine matrix coil. Contrast enhanced 3-dimensional (3D) fast low-angle shot magnetic resonance angiographic sequences, obtained immediately following intravenous administration of 0.1 mmol/kg of contrast, were used to define LA and PV anatomy (echo time 0.8 ms, repetition time 2.2 ms, in-plane resolution 1.4 × 1.4 mm, slice thickness 1.4 mm). To optimize image quality, patients with persistent AF were kept on antiarrhythmic medications and/or referred for cardioversion prior to MRI. LGE MRI scans were acquired within a range of 15 to 25 min (mean 18.8 ± 2.4 min) following 0.2 mmol/kg gadolinium injection (gadopentetate dimeglumine, Bayer Healthcare Pharmaceuticals, Montville, New Jersey) using a fat-saturated 3D inversion recovery-prepared fast spoiled gradient-recalled echo sequence with respiratory navigation and electrocardiographic gating, echo time of 1.52 ms, repetition time of 3.8 ms, in-plane resolution of 1.3 × 1.3, slice thickness of 2.0 mm, and flip angle of 10°. Trigger time for 3D LGE magnetic resonance images was optimized to acquire data during LA diastole. The optimal inversion time was identified with a scout scan (median 270 ms; range 240 to 290 ms) to maximize nulling of LA myocardium. A parallel imaging technique, generalized autocalibrating partially parallel acquisition (reduction factor 2), was used.

IMAGE ANALYSIS. Pre-ablation LGE magnetic resonance images were processed off-line using QMass MR version 7.4 (Medis, Leiden, the Netherlands). Epicardial and endocardial contours were manually drawn around LA myocardium. The reference point was placed at the anterior base of the LA septum, and the LA myocardium in each axial plane was divided into 25 sectors, as seen in **Figure 1**. The image intensity ratio (IIR), a previously described LGE MRI technique that normalizes mean myocardial intensities by the mean intensity of the entire blood pool, was calculated for each sector. The methodology for calculation of the IIR and its association with regional voltage by electroanatomic mapping (EAM) were previously validated (6,8). Interobserver and intraobserver variability of our LA analysis was previously assessed and found to be excellent (6).

MAPPING AND ABLATION PROCEDURE. A double transatrial septal puncture was performed under fluoroscopic guidance. Intravenous heparin was administered to achieve an activated clotting time >350 s. With hemodynamic and electrocardiographic

FIGURE 1 Left Atrial Segmentation and Voltage Correlation

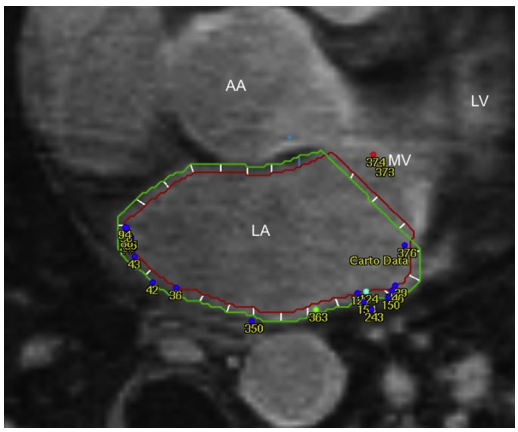

Endocardial and epicardial contours are manually drawn on axial late gadolinium enhancement (LGE) magnetic resonance images. Fast anatomic mapping points are coregistered and projected to LGE magnetic resonance images. Bipolar voltage of each point is correlated to the image intensity ratio of the nearest segment. AA = ascending aorta; LA = left atrium; LV = left ventricle; MV = mitral valve.

monitoring, a 3.5-mm irrigated tip with 2-mm interelectrode spacing ablation catheter (ThermoCool SmartTouch, Biosense Webster) and a decapolar circular mapping catheter, with 25-15 loop diameter, 8-mm interelectrode spacing (LASSO 2515 Variable Loop Eco Nav) were advanced under fluoroscopic guidance to the left atrium. In patients presenting in AF on the day of the procedure, cardioversion was performed prior to image registration and EAM to minimize patient movement and registration errors. If sinus rhythm could not be restored, patients were excluded from analysis. Mapping was performed with an equal distribution of points using a fill threshold of 15 mm, excluding PV ostia. A target of >100 PBP mapping points and >1,000 FAM points was set by consensus at study onset, but the extent of mapping was ultimately left to the operator's discretion. In 19 patients (73%), PBP mapping was performed initially with the ThermoCool SmartTouch ablation catheter and the CARTO3 mapping system (Biosense Webster). In those patients, target contact force >10 *g* was adopted when obtaining points to ensure adequate tissue-catheter contact. The decision to undergo PBP mapping was left to the operator's discretion. LA magnetic resonance angiography was registered to the voltage map by using standard landmark image registration techniques. A detailed fast anatomic map of the entire left atrium was also created with the LASSO Nav catheter and superimposed on pre-existing magnetic resonance images. An internal point filter was used to limit data acquisition to within 5 mm from the anatomic shell to reduce mapping in the blood pool. The ConfiDENSE module, which uses impedance measurement to determine tissue proximity for each electrode, was used to assess electrode-tissue contact during FAM. Intracardiac echocardiography, orthogonal fluoroscopy, and electrogram characteristics were also used to monitor for adequate contact.

After voltage mapping was complete, circumferential lesions were applied surrounding the PV. If conduction from PV to left atrium persisted despite PV isolation, additional lesions were delivered along the original ablation line at sites of earliest activation on the circular mapping catheter. Entrance block into the PVs was confirmed in all patients as the primary procedural endpoint. To prevent short-term recurrences of AF, pre-procedural antiarrhythmic medications were continued for at least 3 months. No immediate post-operative complications were reported.

ABLATION MAP REGISTRATION. FAM-derived voltage maps were registered off-line to pre-ablation LGE images using MASS Research Software (Leiden University Medical Center, Leiden, the Netherlands). Mapping points were extracted from the CARTO workstation and imported into LGE magnetic resonance images using the registration matrix defined during the procedure (Figure 1). An intermediate registration step, performed on ParaView (Kitware, Clifton Park, New York), was needed to reconcile the CARTO coordinate system to the magnetic resonance coordinate system. The mean IIR of the neighboring sector to each mapping point was recorded to evaluate the correlation between bipolar voltage and signal intensity.

FAM AND PBP VOLTAGE COMPARISON. Each of the points acquired during FAM and PBP mapping have coordinates (x, y, and z). For each PBP point, the distances between this point and all FAM points were calculated using a custom-written Python script. PBP points were matched in a 1:1 ratio with FAM points using the shortest orthogonal distance.

STATISTICAL ANALYSIS. Continuous variables are expressed as mean ± SD. Categorical variables are expressed as number (percentage). The unadjusted relationship between IIR and bipolar voltage was initially explored using scatterplots. Because of the skewed nature of bipolar voltage measures, log transformation was used to accommodate modeling within a linear normal framework. A generalized estimating equation (GEE) marginal model with exchangeable working correlation structure was used to examine

TABLE 1 Baseline Patient Characteristics

	Total (N = 26)	Paroxysmal AF (n = 14)	Persistent AF (n = 12)	p Value (Paroxysmal vs. Persistent)
Age, yrs	63.1 ± 7.9	62.3 ± 7.3	64.1 ± 8.8	0.575
Male	19 (73)	10 (71)	9 (75)	0.838
Caucasian	22 (85)	12 (86)	10 (83)	0.867
BMI, kg/m^2	27.2 ± 3.9	26.3 ± 4.9	28.3 ± 2.0	0.199
Hypertension	17 (65%)	10 (71%)	7 (58)	0.484
Diabetes mellitus	1 (4)	0 (0)	1 (8)	0.271
Coronary/vascular disease	4 (15)	2 (14)	2 (17)	0.867
Congestive heart failure	1 (4)	0 (0)	1 (8)	0.271
Prior thromboembolism	2 (8)	2 (14)	0 (0)	0.173
Obstructive sleep apnea	3 (12)	2 (14)	1 (8)	0.636
CHA_2DS_2-VASc score	1.8 ± 1.1	1.9 ± 1.0	1.8 ± 1.2	0.957
0	3 (8)	1 (7)	1 (8)	0.918
1	6 (8)	4 (29)	2 (17)	
2	11 (8)	6 (43)	5 (42)	
3	4 (8)	2 (14)	2 (16)	
4	2 (8)	1 (7)	1 (8)	
5	0 (0)	0 (0)	0 (0)	
6	0 (0)	0 (0)	0 (0)	
AF duration, yrs	4.8 ± 4.3	4.6 ± 3.8	5.0 ± 4.9	0.813
Prior ablations	0.7 ± 0.6	0.6 ± 0.5	0.8 ± 0.7	0.434
0	9 (35)	5 (36)	4 (33)	0.276
1	15 (58)	9 (75)	6 (50)	
2	2 (7)	0 (0)	2 (17)	
Prior ablation strategy				
Radiofrequency ablation	11 (42)	7 (50)	4 (33)	0.565
Cryoballoon ablation	6 (23)	2 (14)	4 (33)	
Smoking				0.532
Never	12 (46)	7 (50)	5 (42)	
Prior	13 (50)	7 (50)	6 (50)	
Current	1 (4)	0 (0)	1 (8)	
DCV pre-mapping	7 (27)	0 (0)	7 (58)	0.0008
LVEF, %	61.0 ± 9.4	65.9 ± 6.1	54.8 ± 9.4	0.002
LA end-systolic area, cm^2	26.8 ± 8.4	24.5 ± 5.9	29.3 ± 10.1	0.157

Values are mean ± SD or n (%).

AF = atrial fibrillation; BMI = body mass index; CHA_2DS_2-VASc = congestive heart failure, hypertension, age ≥75 years, diabetes mellitus, prior stroke, transient ischemic attack, or thromboembolism, vascular disease, age 65-74 years, sex category (female); DCV = direct-current cardioversion; LA = left atrial; LVEF = left ventricular ejection fraction.

the association between bipolar voltage and IIR. The model was clustered by patient and adjusted for age, LA end-diastolic area, sex, body mass index, CHA_2DS_2-VASc score, AF type, AF duration, left ventricular ejection fraction, and history of ablation. Similarly, the correlation between log-transformed PBP voltage and FAM voltage was assessed using an adjusted, patient-clustered GEE marginal model with exchangeable working correlation structure. Receiver-operator characteristic analysis was used to assess the sensitivity and specificity of FAM voltage with PBP-derived fibrosis. Two-sided p values <0.05 were considered to indicate statistical significance. Statistical analysis was performed using STATA version 13 (StataCorp, College Station, Texas).

RESULTS

PATIENT CHARACTERISTICS. We prospectively enrolled 26 patients (19 men [73%], mean age 63.1 ± 7.9 years). Table 1 summarizes the baseline characteristics of patients. Fourteen patients (54%) had paroxysmal AF, and 9 (35%) were undergoing their first ablation procedure. The mean body mass index was 27.2 ± 3.9 kg/m^2, and the median CHA_2DS_2-VASc score was 2 (interquartile range: 1 to 2). Patients with persistent AF had lower left ventricular ejection fractions and higher rates of pre-mapping cardioversion than those with paroxysmal AF; there were no other statistically significant differences between the 2 patient groups.

IMAGE ANALYSIS. MRI studies were performed a median of 1 day (interquartile range: 0 to 6 days) prior to the procedure. Image intensity in arbitrary units and IIR were measured for each sector. The relationship of signal intensity versus IIR and the distribution of each measure are plotted in Online Figure 1. Although image intensity and IIR measures had a linear relationship within each patient, the slope of this association varied across patients, with a range of 7.79 to 75.62 arbitrary units. In contrast to the right-skewed distribution of image intensity, IIR displayed a normal distribution (Figure 2).

CORRELATION OF FAM VOLTAGE AND IIR. Seven of the 26 patients (26%) presented in AF at the beginning of the procedure and required cardioversion prior to mapping. A mean of 734 FAM points (range 397 to 1,089 points) were acquired per patient, and a total of 19,087 points were registered to LGE magnetic resonance images. The average bipolar voltage was 0.88 ± 1.27 mV, and the average IIR was 1.08 ± 0.18. Local IIR was strongly associated with bipolar voltage; however, the relationship was more linear with log transformation of bipolar voltage measures (Figure 2). Using a GEE model, clustered by patient and adjusted for age, sex, CHA_2DS_2-VASc score, AF type, AF duration, previous ablations, LA end-diastolic area, and left ventricular ejection fraction, each unit increase in local IIR was associated with 57% decrease in LA bipolar voltage ($p < 0.0001$) (Table 2). On the basis of unadjusted analyses, local IIR thresholds of >0.74 corresponded to bipolar voltage <0.5 mV.

We performed a stratified analysis in patients with prior ablations versus first-time ablation. The findings are summarized in Online Tables 1 and 2. In brief, mean bipolar voltage was 1.20 mV in ablation-naive patients and 0.78 mV in previously ablated patients. The adjusted relationship between IIR and FAM

FIGURE 2 **Histograms of Distribution of MRI-Signal Intensity and Bipolar Voltage**

(Top) Histogram of signal intensity and image intensity ratio as well as fast-anatomical-mapping and point-by-point bipolar voltage and its log transformation **(middle and bottom panels)**. FAM = fast anatomic mapping; PBP = point-by-point.

voltage was significantly negative in both groups. We also performed a subset analysis of 4 patients with the least percentage of low-voltage mapping points (characterized by voltage ≤0.5 mV). All 4 patients had paroxysmal AF, with a mean bipolar voltage of 1.84 mV and an average proportion of low-voltage points of 8.7 ± 4.1%. As seen in Online Table 3, the adjusted relationship between IIR and FAM-measured bipolar voltage was significantly negative. It was similarly negative upon stratifying mapping points into "normal" voltage (>0.5 mV) and "low" voltage (≤0.5 mV) (Online Tables 4 and 5).

FAM AND PBP VOLTAGE COMPARISON. Serial PBP mapping and FAM were performed in 19 patients. A mean of 82 points per patient were acquired using

TABLE 2 Results of the Generalized Estimating Equation Model

	Univariate		Multivariate	
Log FAM Bipolar Voltage (mV)	**Coefficient**	**p Value**	**Coefficient**	**p Value**
IIR (per U)	−0.90	<0.0001	−0.85	<0.0001
Age (per yr)	−0.03	0.054	−0.01	0.661
Male	−0.60	0.019	−0.53	0.014
BMI (per kg/m^2)	0.06	0.036	0.07	0.004
CHA_2DS_2-VASc score (per U)	−0.02	0.162	−0.13	0.187
Persistent AF	−0.14	0.565	0.02	0.911
Repeat ablation	−0.53	0.027	−0.43	0.026
AF duration (per yr)	−0.05	0.076	−0.06	0.012
LA area (per cm^2)	−0.02	0.162	−0.001	0.952
LVEF (per U %)	0.01	0.415	0.01	0.308

FAM = fast anatomic mapping; IIR = image intensity ratio; other abbreviations as in Table 1.

the PBP technique, and a total of 1,554 points were matched in a 1:1 ratio to the nearest FAM-EAM point. In the matched 1,554 voltage-point pairs, mean PBP voltage was 0.91 ± 0.99 mV, and corresponding mean FAM voltage was 1.20 ± 1.36 mV. Distribution of PBP voltage and its log transformation are displayed in **Figure 2**. A scatterplot of voltage measurements correlating PBP-EAM and FAM-EAM is displayed in Online Figure 2. Using an adjusted, patient-clustered GEE model, log FAM bipolar voltage was significantly associated with log PBP bipolar voltage ($\beta = 0.36$; $p < 0.0001$), as shown in **Table 3**. Individual log PBP versus log FAM voltage linear relationships are demonstrated in Online Figure 3. At low voltages (<40th percentile), the FAM distribution was shifted to the left compared with PBP mapping (**Table 4**). On FAM, the 20th and 40th percentiles were 0.08 and 0.25 mV, respectively, compared with 0.18 and 0.42 mV on PBP mapping. At intermediate voltages (40th to 80th percentiles), FAM and PBP voltages were overlapping (the 60th and 80th percentiles on FAM were 0.69 and 1.52 mV, respectively, vs. 0.73 and 1.54 mV on PBP mapping). At high voltages (>80th percentile), FAM voltage exceeded PBP voltage (the 99th percentile was 6.26 mV on FAM vs. 4.65 mV on PBP mapping). Receiver-operating characteristic analysis of FAM voltage predicting low voltage (<0.5 mV) on PBP mapping showed an area under the curve of 0.75 (Online Figure 4). The FAM voltage with the highest sensitivity and specificity was 0.58 mV (63% sensitivity, 77% specificity).

TABLE 3 Results of the Generalized Estimating Equation Model

	Univariate		Multivariate	
Log Bipolar PBP Voltage (mV)	**Coefficient**	**p Value**	**Coefficient**	**p Value**
Log bipolar FAM voltage (mV)	0.38	<0.0001	0.36	<0.0001
Age (per yr)	0.02	0.382	0.02	0.366
Male	−0.29	0.426	−0.45	0.042
BMI (per kg/m^2)	0.04	0.356	−0.01	0.661
CHA_2DS_2-VASc score (per U)	−0.12	0.428	−0.17	0.244
Persistent AF	−0.25	0.422	−0.08	0.767
Repeat ablation	−0.72	0.004	−0.62	0.033
AF duration (per yr)	−0.01	0.935	0.02	0.518
LA area (per cm^2)	−0.01	0.797	0.01	0.490
LVEF (per U %)	0.02	0.170	0.01	0.510

PBP = point-by-point; other abbreviations as in Tables 1 and 2.

Figure 3 compares IIR maps and FAM and PBP voltage maps in an ablation-naive patient with minimal baseline fibrosis, an ablation-naive patient with posterior wall fibrosis, and a patient with a history of radiofrequency AF ablation. The figure demonstrates a good correlation of LA fibrotic substrate between the 3 modalities. Similarly, Online Figure 5 demonstrates an anterior view of IIR and FAM voltage maps in 2 patients.

DISCUSSION

In this study, we sought to compare LA substrate using different modalities (LGE MRI, FAM, and PBP mapping) in patients presenting for AF ablation. The major findings are as follows: 1) voltage acquired by FAM using a decapolar circular (LASSO 2515 Variable Loop Eco Nav) mapping catheter with a small electrode size correlated with IIR on LGE MRI; and 2) voltage acquired by FAM correlated with voltage on PBP mapping. These findings might have a significant impact on the interpretation of substrate mapping in ablation strategies targeting extra-PV LA remodeling.

FAM VERSUS IIR CORRELATION. A variety of novel AF substrate-mapping approaches have been introduced in recent years, including dominant-frequency analysis (9,10), Shannon entropy (11), complex fractionated electrogram activity (3), focal impulse and rotor modulation (12), bipolar electrogram amplitude (13), and LGE MRI (6-8). Prior studies have shown poor correlation among various techniques (14-17), with the exception of bipolar voltage, which correlates well with LGE MRI (6,7). In a landmark study, Oakes et al. (7) found a positive correlation ($r^2 = 0.61$) between the extent of LGE on MRI with low-voltage zones. Kapa et al. (18) projected EAM points, acquired in sinus rhythm, onto LGE magnetic resonance images and found that mean bipolar voltage in areas of MRI fibrosis was significantly lower than in non-fibrosis areas. In a study by Khurram et al. (6), IIR was used to normalize signal intensities, and intracardiac

TABLE 4 Correlations of Voltage Thresholds Between Voltage-Mapping Modalities

	Percentile					
	5th (95% CI)	20th (95% CI)	40th (95% CI)	60th (95% CI)	80th (95% CI)	99th (95% CI)
FAM voltage	0.03 (0.02–0.03)	0.09 (0.09–0.10)	0.28 (0.27–0.29)	0.69 (0.67–0.71)	1.52 (1.50–1.54)	6.26 (5.99–6.45)
PBP voltage	0.04 (0.03–0.04)	0.18 (0.16–0.20)	0.42 (0.39–0.45)	0.73 (0.68–0.79)	1.54 (1.41–1.67)	4.65 (4.27–4.79)

CI = confidence interval; other abbreviations as in Tables 2 and 3.

mapping points were registered to LGE images. In a multivariate model, each unit increase in IIR was associated with 91.3% decrease in bipolar LA voltage ($p < 0.0001$). In the aforementioned studies, voltage maps were created using PBP acquisition (with or without force sensing). In our investigation, we used a multipolar circular mapping catheter with small electrodes (~1 mm) to acquire a detailed (>1,000 points) voltage maps of the left atrium. In a semi-automated fashion, we were able to merge mapping points onto LGE images and correlate bipolar voltage with neighboring IIR on MRI. Using an adjusted patient-clustered GEE model, each unit increase in local IIR was associated with a 57% decrease in local bipolar LA voltage, demonstrating a good correlation between FAM voltage and IIR in mapping AF substrate.

The distinction between ablation-induced scar and AF-related interstitial fibrosis is an important one to make. On the microscopic level, these represent different pathological processes: necrosis and replacement fibrosis in ablation-related scar and interstitial, diffuse collagen deposition in native AF-related fibrosis. Our group has recently established the distinct characteristics of these processes on LGE MRI (19). Regions with ablation-induced scar exhibit increased contrast uptake (higher IIR), likely signifying higher scar density, compared with regions with native interstitial fibrosis. For these reasons, we performed a stratified analysis in patients with prior ablations versus first-time ablation and found an inverse relationship between IIR and FAM-measured bipolar voltage in both groups.

These findings further demonstrate the utility of MRI in mapping abnormal myocardium as well as guiding AF ablation. In particular, long-term procedural outcomes of patients with persistent AF remain dismal (~50%) (20) and are attributed to extensive atrial fibrotic remodeling not targeted by PV isolation (7,21–23). This is supported by the DECAAF (Delayed-Enhancement MRI Determinant of Successful Radiofrequency Catheter Ablation of Atrial Fibrillation) study, which showed that pre-ablation fibrotic tissue is a major predictor of ablation outcome (21). The efficacy of targeting atrial fibrosis tissue during persistent AF ablation will be assessed in the much awaited DECAAF II study (NCT02529319).

FAM VERSUS PBP CORRELATION. Several studies have shown smaller low-voltage areas and higher mean regional bipolar voltages on FAM compared with PBP mapping (24–26). In line with previous studies, the mean PBP bipolar voltage in our study was 0.91 ± 0.99 mV and mean FAM voltage was 1.20 ± 1.36 mV. Log FAM bipolar voltage was significantly associated with log PBP bipolar voltage ($\beta = 0.36$, $p < 0.0001$). Several factors might influence bipolar voltage amplitude, such as catheter characteristics (electrode size, interelectrode spacing), wave front of activation, electrode-wall contact force, and angle (25,27,28). In fact, our linear ablation catheters had 3.5-mm distal electrodes with interelectrode spacing

FIGURE 3 Illustration of Image Intensity Ratio, FAM-Voltage and PBP-Voltage Maps

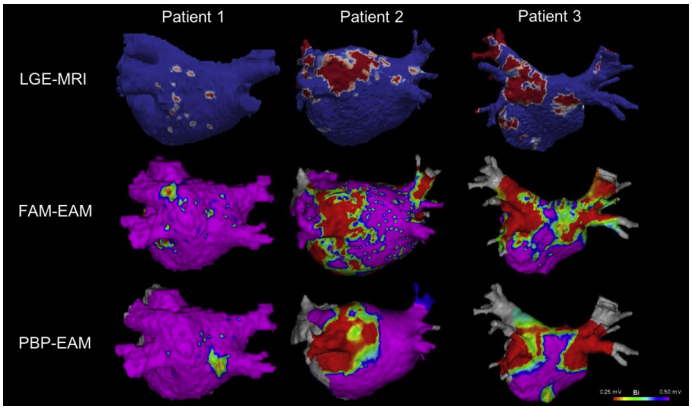

This illustration compares IIR maps **(top)**, FAM voltage maps **(middle)**, and PBP voltage maps **(bottom)** in an ablation-naive patient with minimal baseline fibrosis (Patient #1), an ablation-naïve patient with posterior wall fibrosis (Patient #2), and a patient with a history of prior radiofrequency ablation for AF (Patient #3). The figure demonstrates good correlation between the 3 mapping modalities. Of note, no voltage mapping was done in PV ostia and this area was excluded from any multimodal correlation analysis. Indeed, the thin myocardial sleeves in that area render voltage and magnetic resonance imaging less suited for myocardial substrate mapping. EAM = electroanatomic mapping; FAM = fast anatomic mapping; LGE = late gadolinium enhancement; PBP = point-by-point.

of about 5 mm, whereas multipolar circular catheters had 20 poles, 1-mm electrode size, and 2-6-2-mm interelectrode spacing. Smaller electrode sizes allow increased mapping resolution and a greater ability to discriminate between surviving myocardial fibers and fibrosis; at the same time, smaller electrode size may increase susceptibility of the electrodes to far-field sensing. This was seen on the voltage distribution of the 2 modalities. At low voltages (<40th percentile), the FAM distribution was shifted to the left compared with PBP mapping, which may reflect increased capacity of FAM to detect fibrotic fibers interspaced with normal myocytes, whereas at high voltages (>80th percentile), FAM voltages exceeded PBP voltages (the 99th percentile was 6.26 mV on FAM vs. 4.65 mV on PBP mapping), which may be due to far-field sensing. Moreover, although adequate tissue contact during mapping with the PBP catheter was confirmed by contact force measurement, such data were not available for FAM catheters, which could account for some of the voltage differences.

Voltage mapping in the left atrium is increasingly used to guide AF ablation, the accuracy of which relies heavily on the accurate identification of LA fibrosis (3,29–32). Our work raises awareness of the differences in substrate delineation among various mapping techniques and catheters available that would influence the interpretation of mapped substrate. Based in part on our observations in the present study, our current clinical practice is to use 0.25 to 0.5 mV as a voltage range indicative of abnormal fibrotic tissue and <0.25 mV as consistent with scar when performing either FAM or PBP mapping; in cases in which LGE MRI data are used for scar assessment, we use an IIR value of >1.22 on the basis of equations derived from our work. An important caveat, of course, is that data are lacking regarding how these parameters correlate with scar assessment on the basis of actual tissue evaluation.

STUDY LIMITATIONS. The gold standard in assessing atrial substrate in AF is tissue evaluation. In patients with AF, the muscle bundles were surrounded by thick connective tissue fibers. These thick fibers were also interspaced between the single muscle cells (33). The resolution of PBP or fast anatomic maps using bipolar electrodes is very poor compared with this gold standard, regardless of the mapping density. The fill threshold used by the mapping systems compounds the problem by interpolating areas that are not directly touched by the catheter. Although LGE MRI characterizes the entirety of atrial tissue within each axial slice, the thickness of the slices adds error and interpolation as well. Given the limitations of both EAM and IIR methodologies, in addition to the fact that IIR has not been validated against tissue samples as of yet, the results of this study should be interpreted as 2 methods in relative agreement rather that against a gold standard. This study includes a relatively small cohort of patients who were heterogeneous with regard to prior ablations. However, such heterogeneity did not modify the association between IIR and voltage and demonstrated the wide applicability of LGE MRI in detecting abnormal LA myocardium. Voltage can be affected by tissue contact. Although it cannot be completely ruled out that diminished bipolar voltage on FAM was measured as a consequence of reduced catheter contact (because FAM catheters are not capable of force sensing), it is unlikely to account for the differences between catheters: 1) every attempt was made to ensure adequate contact by means of splaying of the electrodes in contact with the myocardium on fluoroscopy; 2) points were accepted only if they were within 5 mm of the anatomic shell; and 3) patient-clustered association of IIR with voltage suggests that on average, the measures represent LA myocardial tissue characteristics. Our results may also be affected by positional errors when registering ablation points to the magnetic resonance-based segmentation; however, the extent of positional errors appears to be very low on the basis of prior validation studies of our technique (34). For the PBP versus FAM correlation, distances between PBP and FAM points were calculated using the coordinates extracted from CARTO. As such, our results are contingent on having an accurate 3D registration of PBP and FAM-EAM and would be affected by patient movement between the 2 mapping modalities (as seen in individual graphs in **Figure 3**).

CONCLUSIONS

LGE MRI, FAM, and PBP mapping show a good degree of correlation for delineating fibrosis-based AF substrate. Each approach has fundamental technical characteristics, the awareness of which allows proper assessment of electroanatomic AF substrate and potentially avoidance of unnecessary ablation.

ADDRESS FOR CORRESPONDENCE: Dr. Tarek Zghaib, Johns Hopkins University, Division of Cardiology, Carnegie 592, 600 North Wolfe Street, Baltimore, Maryland 21287. E-mail: tzghaib1@jhmi.edu.

PERSPECTIVES

COMPETENCY IN MEDICAL KNOWLEDGE: Substrate modification, targeting low-voltage areas and/or enhancing areas on LGE MRI, has been proposed as an individualized ablation approach. As seen in our study, differences in catheters used for LA substrate mapping may explain the variable results of fibrosis-based ablation strategies. Our findings reflect the importance of adjusting voltage and/or IIR thresholds when examining AF substrate using different modalities.

TRANSLATIONAL OUTLOOK: Intracardiac electrograms and LGE MRI can delineate fibrosis in the left atria of patients with AF, and this study has shown good correlation between the 2 modalities. However, histological confirmation remains of paramount necessity to establish the sensitivity and specificity of these less invasive tools compared with a gold standard. Moreover, a study on healthy volunteers without AF is needed to validate the associations among the various modalities in structurally normal atria.

REFERENCES

1. Calkins H, Kuck KH, Cappato R, et al. 2012 HRS/EHRA/ECAS expert consensus statement on catheter and surgical ablation of atrial fibrillation: recommendations for patient selection, procedural techniques, patient management and follow-up, definitions, endpoints, and research trial design. Europace 2012;14:528–606.

2. Wijffels MC, Kirchhof CJ, Dorland R, Allessie MA. Atrial fibrillation begets atrial fibrillation. A study in awake chronically instrumented goats. Circulation 1995;92:1954–68.

3. Nademanee K, McKenzie J, Kosar E, et al. A new approach for catheter ablation of atrial fibrillation: mapping of the electrophysiologic substrate. J Am Coll Cardiol 2004;43:2044–53.

4. Miyamoto K, Tsuchiya T, Narita S, et al. Bipolar electrogram amplitudes in the left atrium are related to local conduction velocity in patients with atrial fibrillation. Europace 2009;11:1597–605.

5. Morillo CA, Klein GJ, Jones DL, Guiraudon CM. Chronic rapid atrial pacing. Structural, functional, and electrophysiological characteristics of a new model of sustained atrial fibrillation. Circulation 1995;91:1588–95.

6. Khurram IM, Beinart R, Zipunnikov V, et al. Magnetic resonance image intensity ratio, a normalized measure to enable interpatient comparability of left atrial fibrosis. Heart Rhythm 2014;11:85–92.

7. Oakes RS, Badger TJ, Kholmovski EG, et al. Detection and quantification of left atrial structural remodeling with delayed-enhancement magnetic resonance imaging in patients with atrial fibrillation. Circulation 2009;119:1758–67.

8. Khurram IM, Habibi M, Gucuk Ipek E, et al. Left atrial LGE and arrhythmia recurrence following pulmonary vein isolation for paroxysmal and persistent AF. J Am Coll Cardiol Img 2016;9:142–8.

9. Jarman JWE, Wong T, Kojodjojo P, et al. Spatiotemporal behavior of high dominant frequency during paroxysmal and persistent atrial fibrillation in the human left atrium. Circ Arrhythmia Electrophysiol 2012;5:650–8.

10. Guillem MS, Climent AM, Millet J, et al. Noninvasive localization of maximal frequency sites of atrial fibrillation by body surface potential mapping. Circ Arrhythmia Electrophysiol 2013;6:294–301.

11. Ganesan AN, Kuklik P, Lau DH, et al. Bipolar electrogram Shannon entropy at sites of rotational activation. Circ Arrhythmia Electrophysiol 2013;6:48–57.

12. Narayan SM, Krummen DE, Shivkumar K, Clopton P, Rappel W-J, Miller JM. Treatment of atrial fibrillation by the ablation of localized sources. J Am Coll Cardiol 2012;60:628–36.

13. Verma A, Wazni OM, Marrouche NF, et al. Pre-existent left atrial scarring in patients undergoing pulmonary vein antrum isolation. J Am Coll Cardiol 2005;45:285–92.

14. Chrispin J, Gucuk Ipek E, Zahid S, et al. Lack of regional association between atrial late gadolinium enhancement on cardiac magnetic resonance and atrial fibrillation rotors. Heart Rhythm 2016;13:654–60.

15. Ghoraani B, Dalvi R, Gizurarson S, et al. Localized rotational activation in the left atrium during human atrial fibrillation: relationship to complex fractionated atrial electrograms and low-voltage zones. Heart Rhythm 2013;10:1830–8.

16. Viles-Gonzalez JF, Gomes JA, Miller MA, et al. Areas with complex fractionated atrial electrograms recorded after pulmonary vein isolation represent normal voltage and conduction velocity in sinus rhythm. Europace 2013;15:339–46.

17. Schade A, Nentwich K, Costello-Boerrigter LC, et al. Spatial relationship of focal impulses, rotors and low voltage zones in patients with persistent atrial fibrillation. J Cardiovasc Electrophysiol 2016;27:507–14.

18. Kapa S, Desjardins B, Callans DJ, Marchlinski FE, Dixit S. Contact electroanatomic mapping derived voltage criteria for characterizing left atrial scar in patients undergoing ablation for atrial fibrillation. J Cardiovasc Electrophysiol 2014;25:1044–52.

19. Fukumoto K, Habibi M, Gucuk Ipek E, et al. Comparison of preexisting and ablation-induced late gadolinium enhancement on left atrial magnetic resonance imaging. Heart Rhythm 2015;12:668–72.

20. Verma A, Jiang C, Betts TR, et al. Approaches to catheter ablation for persistent atrial fibrillation. N Engl J Med 2015;372:1812–22.

21. Marrouche NF, Wilber D, Hindricks G, et al. Association of atrial tissue fibrosis identified by delayed enhancement MRI and atrial fibrillation catheter ablation: the DECAAF study. JAMA 2014;311:498–506.

22. Cochet H, Mouries A, Nivet H, et al. Age, atrial fibrillation, and structural heart disease are the main determinants of left atrial fibrosis detected by delayed-enhanced magnetic resonance imaging in a general cardiology population. J Cardiovasc Electrophysiol 2015;26:484–92.

23. Xu J, Cui G, Esmailian F, et al. Atrial extracellular matrix remodeling and the maintenance of atrial fibrillation. Circulation 2004;109:363–8.

24. Huemer M, Qaiyumi D, Attanasio P, et al. Does the extent of left atrial arrhythmogenic substrate depend on the electroanatomical mapping technique: impact of pulmonary vein mapping catheter vs. ablation catheter. Europace 2017;19:1293–301.

25. Anter E, Tschabrunn CM, Josephson ME. High-resolution mapping of scar-related atrial arrhythmias using smaller electrodes with closer interelectrode spacing. Circ Arrhythm Electrophysiol 2015;8:537–45.

26. Liang JJ, Elafros MA, Muser D, et al. Comparison of left atrial bipolar voltage and scar using multielectrode fast automated mapping versus point-by-point contact electroanatomic mapping in patients with atrial fibrillation undergoing repeat ablation. J Cardiovasc Electrophysiol 2017;28:280–8.

27. Stinnett-Donnelly JM, Thompson N, Habel N, et al. Effects of electrode size and spacing on the resolution of intracardiac electrograms. Coron Artery Dis 2012;23:126–32.

JACC: CLINICAL ELECTROPHYSIOLOGY VOL. 4, NO. 1, 2018
JANUARY 2018:59–68

28. Ullah W, Hunter RJ, Baker V, et al. Impact of catheter contact force on human left atrial electrogram characteristics in sinus rhythm and atrial fibrillation. Circ Arrhythm Electrophysiol 2015;8:1030–9.

29. Schreiber D, Rieger A, Moser F, Kottkamp H. Catheter ablation of atrial fibrillation with box isolation of fibrotic areas: lessons on fibrosis distribution and extent, clinical characteristics, and their impact on long-term outcome. J Cardiovasc Electrophysiol 2017;28:971–83.

30. Blandino A, Bianchi F, Grossi S, et al. Left atrial substrate modification targeting low-voltage areas for catheter ablation of atrial fibrillation: a systematic review and meta-analysis. Pacing Clin Electrophysiol 2017;40:199–212.

31. Kottkamp H, Berg J, Bender R, Rieger A, Schreiber D. Box isolation of fibrotic areas (BIFA): a patient-tailored substrate modification approach for ablation of atrial fibrillation. J. Cardiovasc. Electrophysiol 2016;27:22–30.

32. Jadidi AS, Lehrmann H, Keyl C, et al. Ablation of persistent atrial fibrillation targeting low-voltage areas with selective activation characteristics. Circ Arrhythmia Electrophysiol 2016;9:e002962.

33. Boldt A, Wetzel U, Lauschke J, et al. Fibrosis in left atrial tissue of patients with atrial fibrillation with and without underlying mitral valve disease. Heart 2004;90:400–5.

34. Dong J, Calkins H, Solomon SB, et al. Integrated electroanatomic mapping with three-dimensional computed tomographic images for real-time guided ablations. Circulation 2006;113:186–94.

KEY WORDS **atrial fibrillation, fibrosis, magnetic resonance imaging, substrate, voltage mapping**

APPENDIX **For supplemental figures and tables, please see the online version of this paper.**